

## A novel additive for rapid and uniform texturing on high-efficiency monocrystalline silicon solar cells

Yongxu Zhang<sup>a,b</sup>, Bolong Wang<sup>b</sup>, Xinpu Li<sup>c</sup>, Zhibo Gao<sup>b</sup>, Ying Zhou<sup>b</sup>, Minghui Li<sup>b</sup>, Danni Zhang<sup>b</sup>, Ke Tao<sup>b</sup>, Shuai Jiang<sup>b</sup>, Huayun Ge<sup>b</sup>, Shaoqing Xiao<sup>a,\*</sup>, Rui Jia<sup>b,\*\*</sup>

<sup>a</sup> Engineering Research Center of IoT Technology Applications (Ministry of Education), Department of Electronic Engineering, Jiangnan University, Wuxi 214122, China

<sup>b</sup> Institute of Microelectronics, Chinese Academy of Sciences, 3# Bei-Tu-Cheng West Road, Beijing, 100029, China

<sup>c</sup> Hanwha-Qcells, Jiangsu, 226200, China



### ARTICLE INFO

#### Index Terms:

Mono-Si  
Pyramid  
Uniform textures  
Additive  
Anisotropic corrosion  
PERC

### ABSTRACT

The wet etching process that produces the textured surface consisting of pyramid structures has been a mature technology for mono-crystalline silicon (mono-Si) solar cells due to the advantages of its low fabrication cost as well as the excellent light trapping effect of such textured surface. Chemical additives such as hazardous solvents like isopropanol are commonly used to effectively assist the fabrication of pyramid structures in addition to the main alkali solution. In this paper, a novel additive that does not contain the hazardous solvents like isopropanol has been developed. The wet etching process using this additive can produce uniform pyramid structures on Si surface in just 7 min, which is at least 3 min shorter than the conventional wet etching process. The composition of this additive is systematically studied and analyzed in terms of the cell performance. We also compare the surface morphology, reflectivity, minority carrier lifetime, quantum efficiency and electroluminescence (EL) of the Si wafers with different textured surface produced by wet etching process using different additives. The results show that such novel additive contributes to the rapid formation of homogeneous small pyramid structures on the Si surface. The open circuit voltage, short circuit current density, fill factor and conversion efficiency of the corresponding passivated emitter and rear cell (PERC) solar cells using such wet etching process are greatly improved, reaching 680 mV, 40.1 mA/cm<sup>2</sup>, 81.3% and 22.18%, respectively.

### 1. Introduction

Solar cell is a kind of semiconductor device that directly converts solar energy into electric energy. Because of its highly mature technology and lower and lower cost, it has been playing an increasingly important role in the new energy industry [1–3]. Industrial crystalline silicon solar cells are mainly divided into polycrystalline silicon (poly-Si) solar cells and monocrystalline silicon (mono-Si) solar cells. Improving the efficiency and reducing the production cost is always the development direction of crystalline silicon solar cells.

Etching special texture on the surface of the silicon wafer with acidic or alkaline chemical reagents is an essential process for crystalline Si solar cells. This greatly reduces the surface reflectivity of the Si wafer, and thus allows the Si wafer to absorb more sunlight and improves the conversion efficiency. For industrial production, poly-metal-assisted chemical etching method is often used to form black silicon structures

on the surface of poly-Si wafer to reduce reflectivity [4,5], while anisotropic etching method is widely used to prepare pyramid structures on mono-Si wafer [6–9]. Such pyramid structures can effectively capture light, and therefore improve the cell performance greatly [10,11].

In general, sodium hydroxide (NaOH) solution and potassium hydroxide (KOH) solution are the most common texturing solutions for the fabrication of such pyramid structures [8,9,11–15]. In order to control pyramid size and uniformity, other chemical reagents such as tetramethyl ammonium hydroxide (TMAH) [16], tribasic sodium phosphate (Na<sub>3</sub>PO<sub>4</sub>·12H<sub>2</sub>O) [17], sodium carbonate and sodium bicarbonate (Na<sub>2</sub>CO<sub>3</sub>/NaHCO<sub>3</sub>) [18] and sodium hypochlorite (NaOCl) [19] have been used instead of NaOH and KOH. Furthermore, some additives are often added to the etching solution to regulate the nucleation process of the pyramid, because these additives can improve the wettability of the wafer surface and control the etching rate [20–22]. Previous reports showed that IPA was often added as an additive in NaOH or KOH-based

\* Corresponding author.

\*\* Corresponding author.

E-mail addresses: [xiaosq@jiangnan.edu.cn](mailto:xiaosq@jiangnan.edu.cn) (S. Xiao), [imesolar@126.com](mailto:imesolar@126.com) (R. Jia).

texturing systems [15,23]. However, IPA is easy to volatilize at high temperature, which reduces its concentration in the mixed solution and leads to unstable textures made in subsequent batches. Moreover, IPA gases and waste liquids are harmful and difficult to dispose of. Therefore, some other improvement measures and new additives have gradually entered people's field of vision. For example, adding potassium silicate ( $K_2SiO_3$ ) to KOH and IPA systems can reduce pyramid size and shorten texturing time [15]. By using metal-assisted chemical etching method to etch nano-structures on the surface of the silicon wafer and then immersing the wafer into a NaOH-based solution with low concentration of IPA, the nucleation time of pyramids was shortened to 10 min and the resultant pyramid was about 3  $\mu m$  in size [11]. Gong et al. used some special additives containing  $C_{12}H_{25}NHCH_2CH_2COO-Na$  and  $C_{32}H_{58}O_{10}$  to obtain small round pyramids [21].

In this work, a new additive has been developed. By changing the anisotropic etching characteristics in the etching process of mono-Si, the texturing time was further shortened to 7 min, which may greatly promote the production efficiency of mono-Si solar cells without decreasing the conversion efficiency. In addition, the main components of the additive are systematically studied and optimized. Finally, uniform and dense small-sized pyramid texture are obtained by adding the optimal additive into the solution during texturing. The width of the pyramid is about 2  $\mu m$  and the height is about 1.5  $\mu m$ . The weighted average reflectance of the treated silicon wafer can be as low as 8.7%, within the test wavelength range of 375–1100 nm. The corresponding passivated emmitter and rear cells give an average efficiency ( $\eta$ ) of 22.18%. The average open circuit voltage ( $V_{oc}$ ), short circuit current density ( $J_{sc}$ ), and Fill Factor (FF) are greatly improved, reaching 680 mV, 40.1 mA/cm<sup>2</sup> and 81.3% respectively. Therefore, the additive developed in this work has a promising market prospect in photovoltaic industry.

## 2. Experimental

Commercial p-type diamond wire sawing mono-Si wafers were used in this experiment with a size of  $156.75 \times 156.75 mm^2$ , a thickness of  $180 \pm 20 \mu m$  and a resistivity of  $0.5\text{--}1.5 \Omega cm$ . Fig. 1 is the schematic diagram of the experimental steps. Firstly, KOH solution was used to remove the saw damage layers and amorphous silicon (a-Si) layers sawn by diamond wire on the surface of the mono-Si wafers. Due to the existence of a-Si layers, it is difficult for pyramid to distribute uniformly on the surface of the silicon wafers [23]. Secondly, the samples were immersed in a 80 °C deionized water solution containing 2 wt% KOH and 1 vol% additive. The textured wafers were then made into passivated emitter and rear cell (PERC) solar cells by standard production process, including phosphorus diffusion, phosphosilicate glass (PSG) removal, rear PN junction polishing, rear passivation by  $Al_2O_3$ , front SiNx film coating by PECVD, rear laser ablation, screen printing and firing for metal contact.

In order to measure the minority carrier lifetime, semi-finished Si wafers subjected to saw damage removal, the textured process, two-sided phosphorus diffusion, two-sided PSG removal and two-sided PECVD SiNx deposition were prepared as shown in Fig. 2. Surface morphology was characterized by scanning electron microscopy (SEM, Hitachi, S4800). The minority carrier lifetime was measured by quasi-steady-state photo-conductance method with a Sinton WCT-120. The surface lifetime mapping was conducted by Semilab PV-2000. Reflectance was measured by Incident Photon to Charge Carrier Efficiency (IPCE) of solar cells measurement system (IBS-SYSCOS). Internal quantum efficiency (IQE) and external quantum efficiency (EQE) were measured by IPCE of solar cells measurement system (Sofn, 7-SCSpec, China). Electroluminescence image was measured by EL sorting machine (zhewei, SA-220, China).

## 3. Results and Discussion

The chemical equation for anisotropic etching of crystalline silicon in

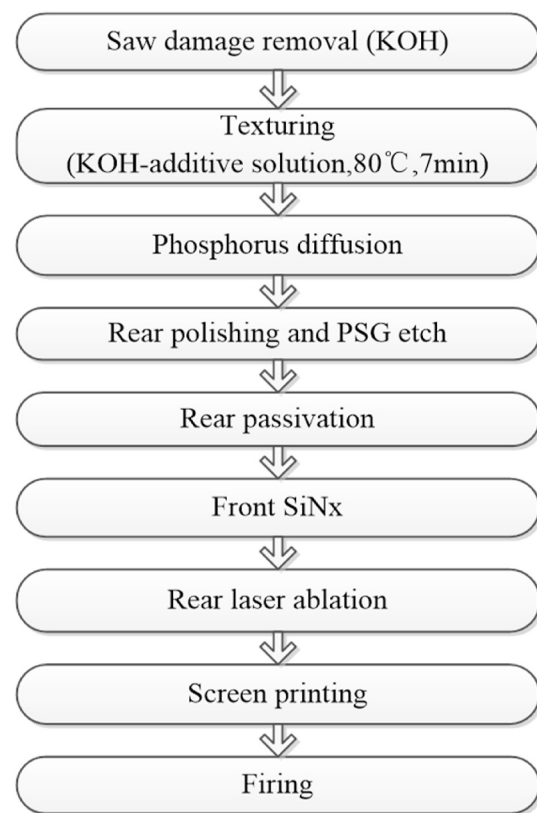


Fig. 1. Schematic diagram of PERC process.

alkaline solution is as follows Eq 1 [7,9]:



In alkaline solution, the etching rate of mono-Si in (100) plane and (111) plane is different, which mainly depends on the number of dangling bonds per unit area of different crystal planes [21]. Fig. 3 shows the schematic diagram of silicon atoms in different crystal planes. For (111) plane, each silicon atom connects one dangling bond and three covalent bonds, while for (100) plane, each silicon atom connects two dangling bonds and two covalent bonds. Obviously, the number of dangling bonds on the (100) plane is more than that on the (111) plane. When removing a silicon atom from (100) plane, two covalent bonds need to be broken, while for (111) plane, three covalent bonds need to be broken. So the etching rate on the (100) plane is higher than that on the (111) plane, and this difference in etching rate between the two crystal planes finally forms pyramid structures on the crystalline silicon surface [21].

In this work, we develop an additive that can greatly help reduce the texturing time. The additive contains a special organic macromolecular surfactant-sodium lignosulfonate (0.4 wt% at default), Cyclodextrin (5 wt%) and  $Na_2CO_3$  (3 wt%). Fig. 4 shows the SEM images of the silicon wafers at different texturing times. It is clear that both the size and number of pyramids increase with the reaction time. When the reaction time is short, the size of the pyramid is less than 1  $\mu m$  and the distribution is uneven. This can be defined as "primary stage" of pyramid nucleation. From Fig. 4(a) with texturing time of 3 min, one can see that there are a large number of irregular overlapping pyramids and several large flat areas not covered by any pyramid structures. With the increase in texturing time to 5 min (Fig. 4(b)), the silicon surface is consisting of a large number of small pyramids with uneven distribution and several small flat areas covered by no pyramid structures. When the texturing time is once exceeding 7 min like Fig. 4(c) and (d), the silicon surface is almost completely covered by all pyramids. However, excessive

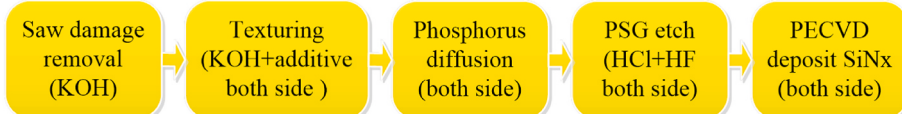


**Fig. 2.** The fabrication process of semi-finished Si wafers for minority carrier lifetime measurement.

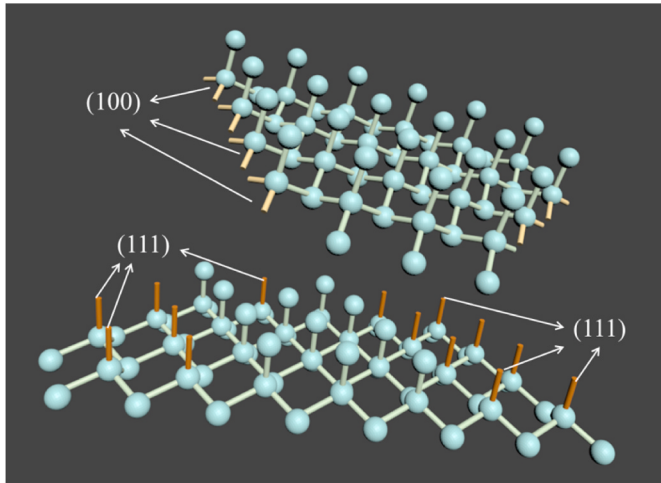


**Fig. 3.** Schematic diagram of mono-Si surface with (100) and (111) crystal planes.

texturing like 11 min shown in Fig. 4(e) may still increase the pyramid size but lead to over etching, as marked by the circle in Fig. 4(e).

**Table 1** shows the weighted average reflectivity of the silicon wafers at different texturing times under the standard condition of AM1.5 within the test wavelength range of 375–1000 nm. The weighted average reflectivity is calculated by the Eq 2 [24,25]:

$$R_a = \frac{\int_{375}^{1000} R(\lambda)N(\lambda)d\lambda}{\int_{375}^{1000} N(\lambda)d\lambda} \quad (2)$$

where  $R(\lambda)$  is the total reflectivity and  $N(\lambda)$  is the solar flux under AM1.5 standard conditions. As can be seen from **Table 1**, with the

increase in etching time, the reflectivity first decreases greatly and reaches a minimum of 12.35% at 9 min, although the reflectivity of 12.61% at 7 min is quite close to that at 9 min. With the further increase in etching time, the reflectivity turns to increase slightly due to the over etching. In combination with both SEM and reflectivity results, we can conclude that the optimum texturing time is 7–9 min.

In both Fig. 4(c) and (d), although the pyramids cover the Si surface completely but their size varies greatly from 1  $\mu\text{m}$  to 5  $\mu\text{m}$ . Furthermore, these pyramids are not uniformly distributed over the surface. Therefore, we systematically study the effect of the content of sodium ligninsulfonate on the textured surface. Four different content of sodium ligninsulfonate (0.4 wt%, 0.6 wt%, 0.8 wt% and 1.0 wt%), are respectively named after Additive A, B, C and D. The detailed content of sodium ligninsulfonate, cyclodextrin and  $\text{Na}_2\text{CO}_3$  are listed in **Table 2**. The SEM images of the silicon wafers subjected to 7 min's anisotropic etching with different additives are shown in Fig. 5. It is clear that both the pyramid size and height gradually decrease with the increase in the

**Table 1**

The weighted average reflectivity of the silicon wafers at different texturing times within the test wavelength range of 375–1000 nm.

Time (min)	3	5	7	9	11
Weighted average reflectivity (%)	20.37	15.72	12.61	12.35	12.77

**Table 2**

The main ingredients of four additives.

	Sodium ligninsulfonate	Cyclodextrin	$\text{Na}_2\text{CO}_3$
Additive A	0.4 wt%	5 wt%	3 wt%
Additive B	0.6 wt%	5 wt%	3 wt%
Additive C	0.8 wt%	5 wt%	3 wt%
Additive D	1 wt%	5 wt%	3 wt%

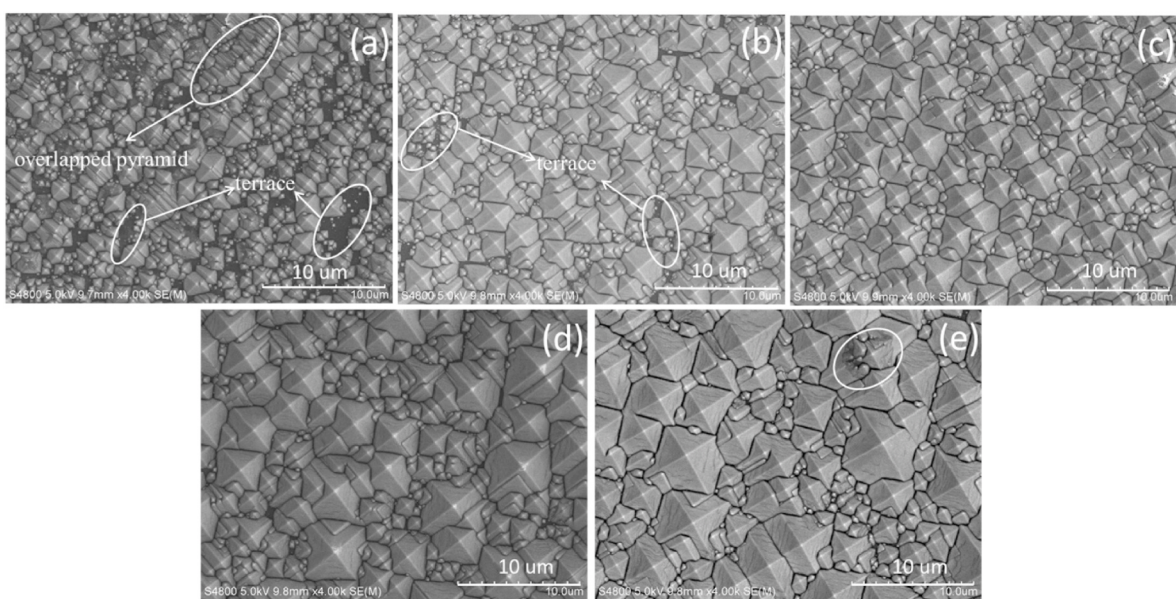


**Fig. 4.** The SEM images of silicon wafers at different texturing times: (a) 3 min; (b) 5 min; (c) 7 min; (d) 9 min; (e) 11 min.

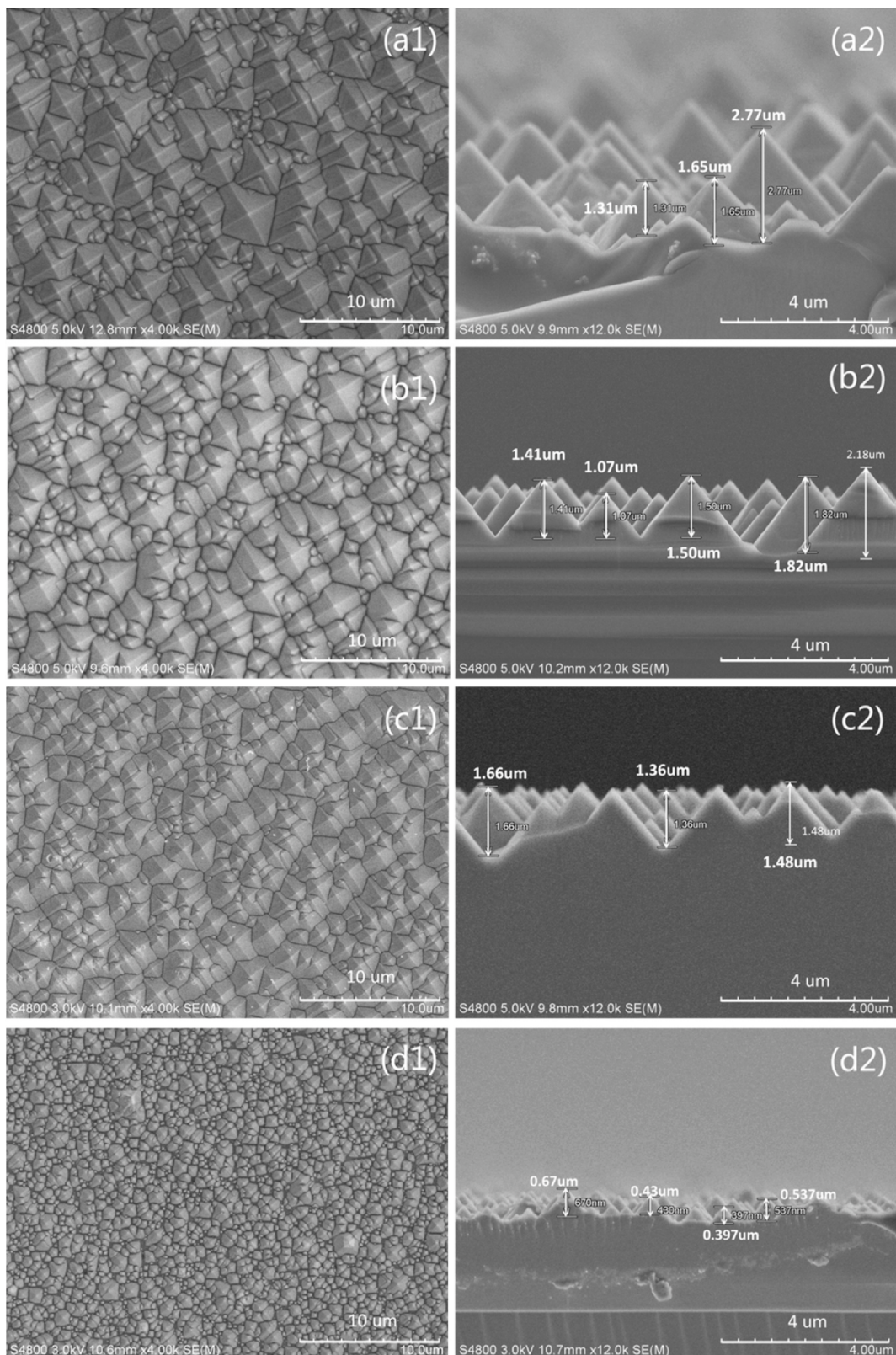


**Fig. 5.** Surface morphologies and corresponding cross-sectional views of the silicon wafers textured by for different solutions: (a1) and (a2) Additive A; (b1) and (b2) Additive B; (c1) and (c2) Additive C; (d1) and (d2) Additive D.

content of sodium ligninsulfonate. For Additive A, both the pyramid size and height vary greatly as observed in Fig. 4. However, with the increase in the content of sodium ligninsulfonate, the uniformity of these pyramids is significantly improved as shown in Fig. 5(b) and (c). In

particular, the pyramid size is about 2 μm and the height is 1.5 μm for Additive C. Furthermore, with the further increase in the content of sodium ligninsulfonate (like Additive D), both the pyramid size and height can reduce to about 0.5 μm.

This can be well understood since the sulfonic group contained in the sodium lignosulfonate molecule can be combined with the dangling bonds of the silicon atoms, thus reducing the probability of the silicon atoms reacting with  $\text{OH}^-$ . Excessive sodium ligninsulfonate may seriously prevent the dangling bonds of silicon atoms from reacting with  $\text{OH}^-$ , thus making the pyramid size extremely small like less than 1  $\mu\text{m}$  as shown in Fig. 5(d). In other words, sodium ligninsulfonate, as a surfactant, can effectively control the etching rate and tune the pyramid size. Appropriate content of sodium ligninsulfonate in the additive can make the nucleation points compact, dense and uniform.

The reflectivity curve and weighted average reflectivity of the samples textured by four additives before and after  $\text{SiN}_x$  deposition are shown in Fig. 6 and Table 3 respectively. Compared with raw-Si, the pyramid structure on the silicon wafer can greatly reduce the reflectivity of the front surface. In addition, the silicon wafers treated with Additive D have a much higher reflectivity than those treated with other three additives. Because there are many non-etched areas on the wafers, it is difficult for pyramid to form multiple reflections, and the light trapping is not effective. The reflectivity curves of the silicon wafers textured by Additives B and C are relatively close. The uniform and dense small pyramid obtained by using Additive C can realize maximum front surface light absorption [26], and its weighted average reflectivity is as low as 8.7%. After deposition of  $\text{SiN}_x$  by PECVD, the weighted average reflectivity of group C is also the lowest (1.3%) of the four samples (see Table 3).

The uniformity of the texture can be further verified by minority carrier lifetime. The textured wafers are made into semi-finished Si wafers for minority carrier lifetime (mapping) measurement [27]. The mappings of minority carrier lifetime, the minority carrier lifetime and corresponding recombination rate measured by PV 2000 are shown in Fig. 7 and Table 4, respectively. From both Fig. 7 and Table 4, it is clear that the minority carrier lifetimes for Additive C and D are higher than those for Additive A and B. From the mapping pictures shown in Fig. 7, one can conclude that the minority carrier lifetime mapping picture for Additive C is the most uniform one with high minority carrier lifetime values since it is mostly consisting of purple and blue regions with higher minority carrier lifetime values and the green regions with lower minority carrier lifetime values are extremely rare. The highest minority carrier lifetime value for Additive D is slightly larger than that for Additive C. This may be due to the existence of many unetched areas with better surface passivation effect for the silicon wafers treated by Additive D.

We also measure the minority carrier lifetime and the auger recombination rate using Sinton WCT-120, and the results are presented

**Table 3**

The weighted average reflectivity of the silicon wafers textured by four different additives before and after  $\text{SiN}_x$  deposition within the test wavelength range of 375–1000 nm.

Items	Raw-Si	Additive A	Additive B	Additive C	Additive D
Before deposition of $\text{SiN}_x$	44.85	12.87	10	8.7	17.91
After deposition of $\text{SiN}_x$		3.13	2.26	1.3	5.96

in Fig. 8. The variation trend with the increase of the content of sodium ligninsulfonate (from Additive A to Additive D) is in good agreement with the above results. The semi-finished Si wafers textured by both Additive C and D possess the highest minority carrier lifetime values and the lowest auger recombination rates at a carrier density injection level of  $1 \times 10^{15}/\text{cm}^3$ . For the semi-finished Si wafers textured by Additive A and B, the large-sized pyramids may have larger surface area, more defect and recombination centers, resulting in the decrease of minority carrier lifetime and the increase of recombination rate as well [28,29]. Furthermore, the height of the pyramid structures formed by Additive A is quite different, which may lead to non-uniform thickness of deposited  $\text{SiN}_x$  passivation layer, further deteriorating the passivation performance.

The cell performance including conversion efficiency ( $\eta$ ), open circuit voltage ( $V_{oc}$ ), short circuit current density ( $J_{sc}$ ) and fill factor (FF) of the PERC cells textured by four different additives are compared in Table 5. Also, both external quantum efficiency (EQE) and internal quantum efficiency (IQE) curves of these corresponding PERC cells are displayed in Fig. 9. It is obvious that the PERC cells textured by Additive C have the highest  $V_{oc}$  (680 mV), the highest  $I_{sc}$  (40.1  $\text{mA}/\text{cm}^2$ ), the highest  $\eta$  (22.18%), the highest EQE and the highest IQE. This can be attributed to the fact that the Si wafers textured by Additive C possess uniform and dense small-sized pyramid structures, which could not only absorb more sunlight but also promote good surface passivation effect [30,31].

Electroluminescence (EL) spectrum is usually used to characterize the relationship between potential recombination defects, minority carrier diffusion length and emission intensity. The EL spectra of the PERC solar cells textured by different additives are presented in Fig. 10. One can observe from Fig. 10(a) and (b) many distinct black spots for the PERC cells textured by Additive A and B. In contrast, the EL spectra are quite uniform and free from black spots for the PERC cells textured by Additive C and D. These results further verify that the PERC cells

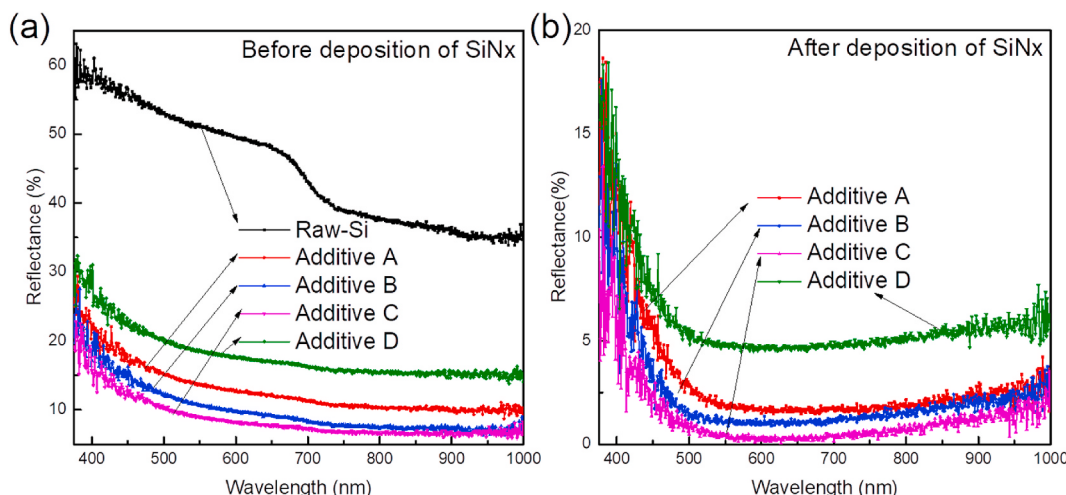


**Fig. 6.** Reflectivity curves of the silicon wafers textured by four different additives: (a) Before and (b) after deposition of  $\text{SiN}_x$  by PECVD. (For interpretation of the references to colour in this figure legend, the reader is referred to the Web version of this article.)

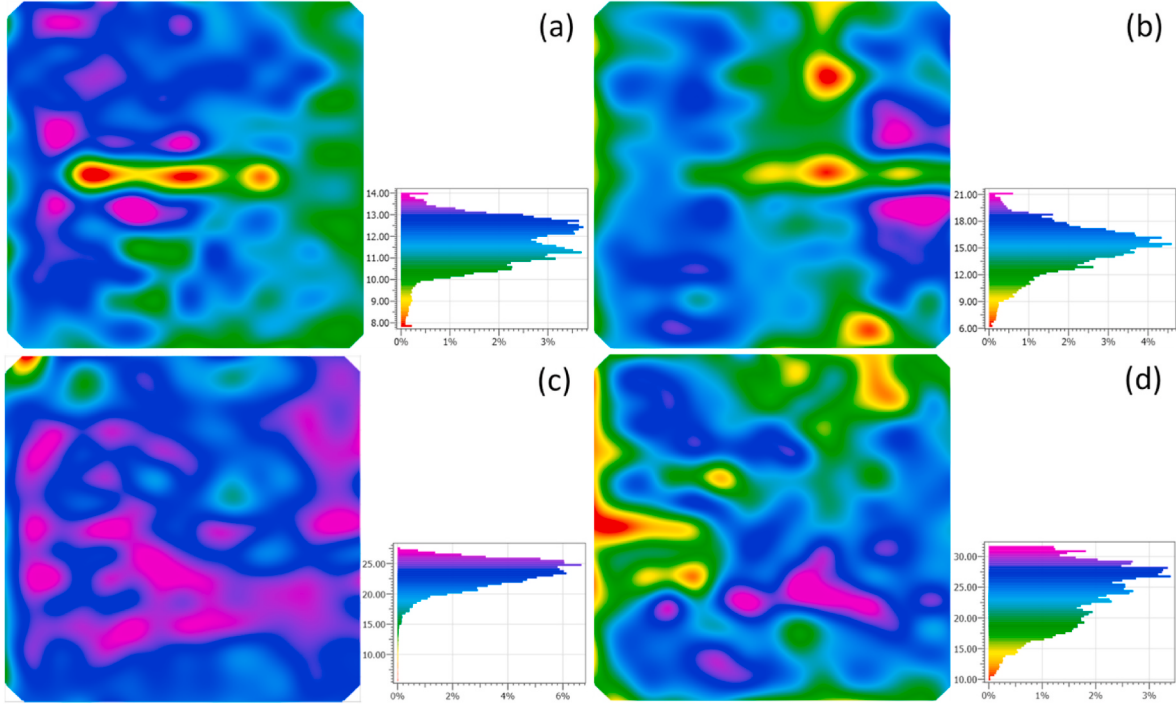


**Fig. 7.** The effective minority carrier lifetime mappings of semi-finished Si wafers textured by (a) Additive A, (b) Additive B, (c) Additive C and (d) Additive D.

**Table 4**

Minority carrier lifetime and corresponding recombination rate of semi-finished Si wafers ( $156.75 \times 156.75 \text{ mm}^2$ ) textured by four different additives.

Items	$S_{\text{Ave}}(\text{cm/s})$	$\tau_{\text{Ave}}(\mu\text{s})$	$\tau_{\min}(\mu\text{s})$	$\tau_{\max}(\mu\text{s})$
Additive A	775.86	11.72	7.86	14.07
Additive B	627.65	14.96	6.26	21.33
Additive C	394	23.38	5.78	27.87
Additive D	286.63	26.85	9.98	31.9

textured by Additive C with uniform and dense small-sized pyramid structures possess the best cell performance.

#### 4. Conclusion

In summary, we develop a novel additive consisting of sodium

**Table 5**

Cell performance of the PERC solar cells ( $156.75 \times 156.75 \text{ mm}^2$ ) textured by four different additives.

Items	$\eta(\%)$	$V_{\text{oc}}(\text{mV})$	$J_{\text{sc}}(\text{mA/cm}^2)$	$\text{FF}(\%)$
Additive A	21.84	673	40	81
Additive B	21.96	675	39.95	81.42
Additive C	22.18	680	40.1	81.3
Additive D	21.49	671	39.52	81

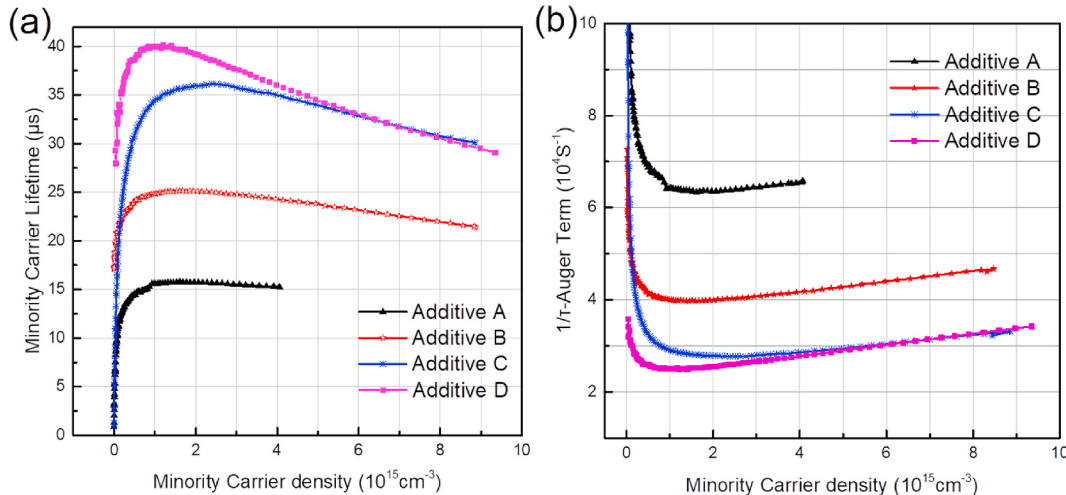


**Fig. 8.** (a) Minority carrier lifetime and (b) auger recombination rate as a function of the injection level measured by Sinton WCT-120 for the semi-finished Si wafers textured by four different additives.

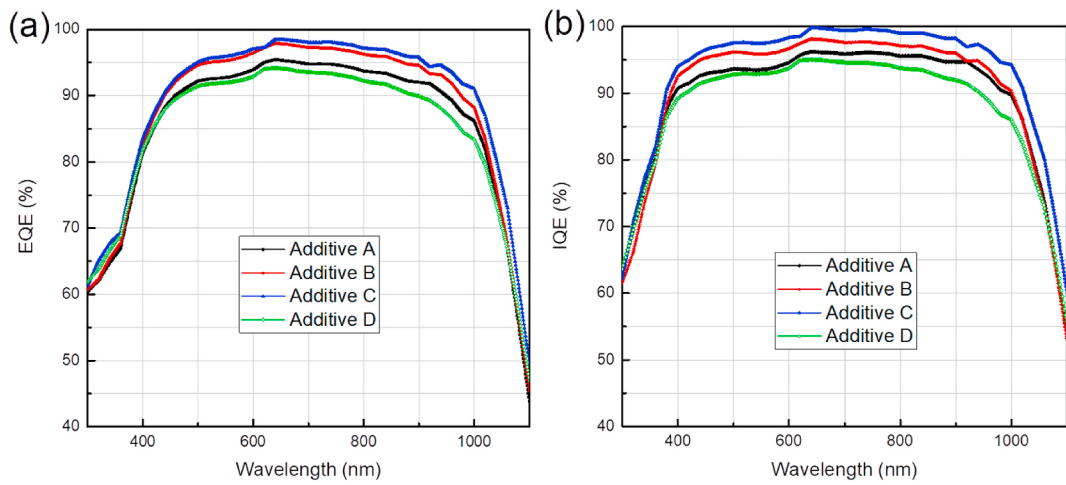


**Fig. 9.** (a) EQE and (b) IQE curves of the PERC solar cells textured by four different additives.

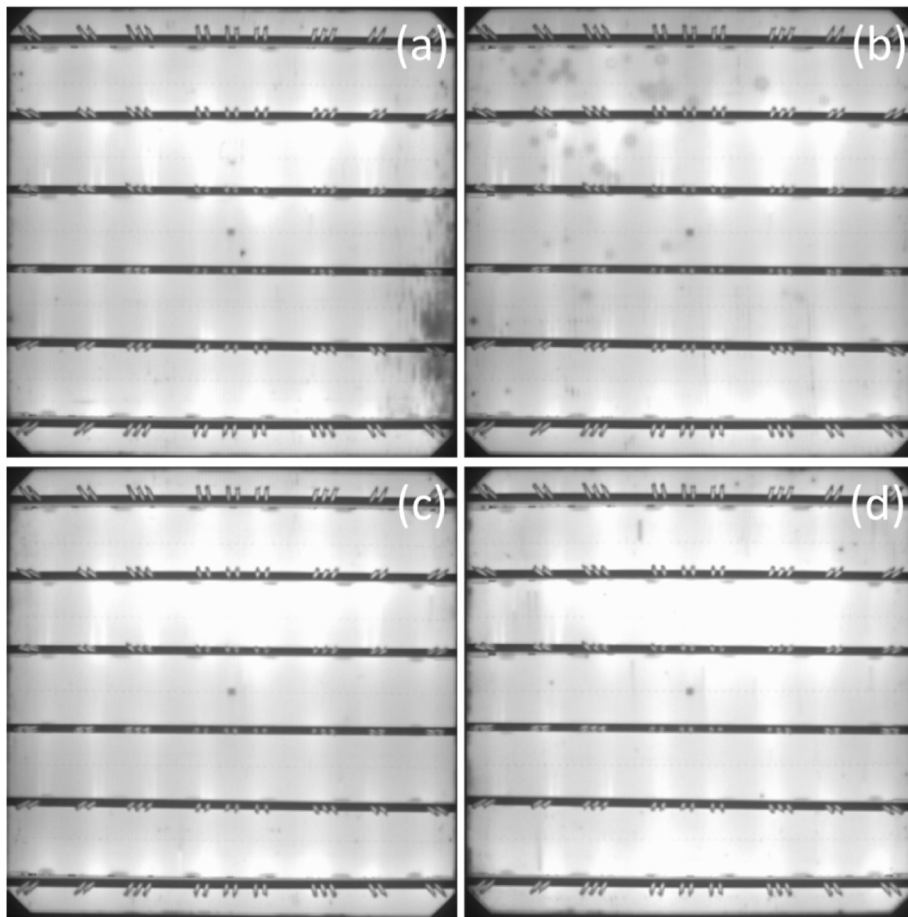


**Fig. 10.** EL image of the PERC solar cells textured by four different additives: (a) Additive A; (b) Additive B; (c) Additive C; (d) Additive D.

ligninsulfonate, cyclodextrin and sodium carbonate without any hazardous solvents like isopropanol. The wet etching process using this additive can produce uniform pyramid structures on Si surface in just 7 min, which is at least 3 min shorter than the conventional wet etching process. We systematically study the composition of sodium ligninsulfonate on the surface morphology, reflectivity, minority carrier lifetime, quantum efficiency, EL and cell performance of the Si wafers or the PERC Si cells. The results show that the additive (Additive C) consisting of 0.8 wt% sodium ligninsulfonate, 5 wt% cyclodextrin and 3 wt%

sodium carbonate possess the best performance. The open circuit voltage, short circuit current density, fill factor and conversion efficiency of the corresponding PERC solar cells using such wet etching process are greatly improved, reaching 680 mV, 40.1 mA/cm<sup>2</sup>, 81.3% and 22.18%, respectively. Such novel additive contributes to the rapid formation of homogeneous and dense small-sized pyramid structures on the Si surface, which greatly promote the cell performance in terms of enhanced light absorption and surface passivation effect.

## CRediT authorship contribution statement

**Yongxu Zhang:** Validation, Data curation, Formal analysis, Investigation, Writing - original draft, Writing - review & editing. **Bolong Wang:** Validation, Data curation. **Xinpu Li:** Investigation. **Zhibo Gao:** Investigation. **Ying Zhou:** Validation. **Minghui Li:** Investigation. **Danni Zhang:** Investigation. **Ke Tao:** Software, Supervision. **Shuai Jiang:** Software, Supervision. **Huayun Ge:** Investigation. **Shaoqing Xiao:** Methodology, Data curation, Writing - original draft, Writing - review & editing, Project administration. **Rui Jia:** Conceptualization, Data curation, Writing - review & editing, Project administration.

## Declaration of competing interest

The authors declare that they have no known competing financial interests or personal relationships that could have appeared to influence the work reported in this paper.

## ACKNOWLEDGEMENTS

This work is supported by the National Natural Science Foundation of China under Grants 62074070, 51702355 and 61804108, the National Key Research and Development Program of China under Grants 2018YFB1500500 and 2018YFB1500200 and JKW project 31512060106, Natural Science Foundation of Beijing Municipality under Grant 4192064, the Fundamental Research Funds for the Central Universities of China under Grant JUSRGP51726B, the 111 Project under Grant B12018.

## References

- [1] World energy outlook 2017 China special report released in Beijing, China Oil Gas 25 (97.01) (2018) 44–46.
- [2] M.H. Alaaeddin, et al., Photovoltaic applications: status and manufacturing prospects, Renew. Sustain. Energy Rev. 102 (2019) 318–332.
- [3] S. Danlami Musa, et al., China's energy status: a critical look at fossils and renewable options, Renew. Sustain. Energy Rev. 81 (2018) 2281–2290.
- [4] Xinpu Li, et al., High-efficiency multi-crystalline black silicon solar cells achieved by additive assisted Ag-MACE, Sol. Energy 195 (2020) 176–184.
- [5] Xiaowan Dai, et al., The influence of surface structure on diffusion and passivation in multicrystalline silicon solar cells textured by metal assisted chemical etching (MACE) method, Sol. Energy Mater. Sol. Cell. 186 (2018) 42–49.
- [6] Eva Vazsonyi, et al., Improved anisotropic etching process for industrial texturing of silicon solar cells, Sol. Energy Mater. Sol. Cell. 57 (2) (1999) 179–188.
- [7] H. Seidel, et al., Anisotropic etching of crystalline silicon in alkaline solutions I. Orientation dependence and behavior of passivation layers, J. Electrochem. Soc. 137 (11) (1990) 3612–3626.
- [8] Sami Iqbal, et al., Highly efficient and less time consuming additive free anisotropic etching of silicon wafers for photovoltaics, Silicon 12 (4) (2020) 773–778.
- [9] Hussien A. Motaweh, Alkali anisotropic chemical etching of p-silicon wafer. International Conference on Mechanics, Materials and Structural Engineering (ICMMSE 2016), Atlantis Press, 2016.
- [10] Quntao Tang, et al., Efficient light trapping of quasi-inverted nanopyramids in ultrathin c-Si through a cost-effective wet chemical method, RSC Adv. 6 (99) (2016) 96686–96692.
- [11] Jiale Yang, et al., Nanostructure-induced fast texturization of mono-crystalline silicon in low-concentration alkaline solution, Mater. Sci. Semicond. Process. 94 (2019) 1–8.
- [12] Galib Hashmi, et al., Texturization of as-cut p-type monocrystalline silicon wafer using different wet chemical solutions, Appl. Phys. A 124 (6) (2018).
- [13] Yingli Cao, et al., Fabrication of silicon wafer with ultra low reflectance by chemical etching method, Appl. Surf. Sci. 257 (17) (2011) 7411–7414.
- [14] N. Bachtouli, et al., Implications of alkaline solutions-induced etching on optical and minority carrier lifetime features of monocrystalline silicon, Appl. Surf. Sci. 258 (22) (2012) 8889–8894.
- [15] Prabir Kanti Basu, et al., Liquid silicate additive for alkaline texturing of mono-Si wafers to improve process bath lifetime and reduce IPA consumption, Sol. Energy Mater. Sol. Cell. 113 (2013) 37–43.
- [16] P. Papet, et al., Pyramidal texturing of silicon solar cell with TMAH chemical anisotropic etching, Sol. Energy Mater. Sol. Cell. 90 (15) (2006) 2319–2328.
- [17] U. Gangopadhyay, et al., A novel low cost texturization method for large area commercial mono-crystalline silicon solar cells, Sol. Energy Mater. Sol. Cell. 90 (20) (2006) 3557–3567.
- [18] Amada Montesdeoca-Santana, et al., Ultra-low concentration Na<sub>2</sub>CO<sub>3</sub>/NaHCO<sub>3</sub> solution for texturization of crystalline silicon solar cells, Prog. Photovoltaics Res. Appl. 20 (2) (2012) 191–196.
- [19] Linfeng Sun, Jiuyao Tang, A new texturing technique of monocrystalline silicon surface with sodium hypochlorite, Appl. Surf. Sci. 255 (22) (2009) 9301–9304.
- [20] Jaehyeong Lee, et al., Optimization of fabrication process of high-efficiency and low-cost crystalline silicon solar cell for industrial applications, Sol. Energy Mater. Sol. Cell. 93 (2) (2009) 256–261.
- [21] Xiao Tong Gong, et al., New surface microstructure of mono-si wafer textured using wet chemical solutions for solar cell, Appl. Phys. A 125 (7) (2019).
- [22] S.A. Campbell, et al., Inhibition of pyramid formation in the etching of Si p (100) in aqueous potassium hydroxide-isopropanol, J. Micromech. Microeng. 5 (3) (1995) 209–218.
- [23] Prabir Kanti Basu, et al., Novel low-cost alkaline texturing process for diamond-wire-sawn industrial monocrystalline silicon wafers, Sol. Energy Mater. Sol. Cell. 185 (2018) 406–414.
- [24] Guoyu Su, et al., The influence of black silicon morphology modification by acid etching to the properties of diamond wire sawn multicrystalline silicon solar cells, IEEE J. Photovolt. 8 (4) (2018) 937–942.
- [25] B.S. Akila, et al., Investigations on the correlation between surface texturing histogram and the spectral reflectance of (100) Crystalline Silicon Substrate textured using anisotropic etching, Sens. Actuator A-Phys. 263 (2017) 445–450.
- [26] Shengyao Yang, Peiqi Ge, Lei Zhang, The effects of different parameters of pyramidal textured silicon surface on the optical reflectance, Sol. Energy 134 (2016) 392–398.
- [27] J.A. Giesecke, et al., Minority carrier lifetime imaging of silicon wafers calibrated by quasi-steady-state photoluminescence, Sol. Energy Mater. Sol. Cell. 95 (3) (2011) 1011–1018.
- [28] Simeon C. Baker-Finch, et al., The contribution of planes, vertices, and edges to recombination at pyramidal textured surfaces, IEEE J. Photovolt. 1 (1) (2011) 59–65.
- [29] Minkyu Ju, et al., The effect of small pyramid texturing on the enhanced passivation and efficiency of single c-Si solar cells, RSC Adv. 6 (55) (2016) 49831–49838.
- [30] Prabir Kanti Basu, et al., The effect of front pyramid heights on the efficiency of homogeneously textured inline-diffused screen-printed monocrystalline silicon wafer solar cells, Renew. Energy 78 (2015) 590–598.
- [31] Minkyu Ju, et al., Influence of small size pyramid texturing on contact shading loss and performance analysis of Ag-screen printed mono crystalline silicon solar cells, Mater. Sci. Semicond. Process. 85 (2018) 68–75.